MOLECULAR IMAGING AND BIOLOGY

Mol Imaging Biol (2017) 19:610–616
DOI: 10.1007/s11307-016-1022-1

Published Online: 9 November 2016

RESEARCH ARTICLE

Effects of an Unlabeled Loading Dose on Tumor-Specific Uptake of a Fluorescently Labeled Antibody for Optical Surgical Navigation

Lindsay S. Moore,[1] Eben L. Rosenthal,[2] Esther de Boer,[1,3] Andrew C. Prince,[1] Neel Patel,[1] Joshua M. Richman,[4] Anthony B. Morlandt,[5] William R. Carroll,[1] Kurt R. Zinn,[6] Jason M. Warram[1,6,7]

[1]*Department of Otolaryngology, University of Alabama at Birmingham, Birmingham, AL, USA*
[2]*Department of Otolaryngology, Stanford University, Stanford, CA, USA*
[3]*Department of Surgery, University of Groningen, Groningen, the Netherlands*
[4]*Department of Surgery, University of Alabama at Birmingham, Birmingham, AL, USA*
[5]*Department of Oral & Maxillofacial Surgery, University of Alabama Birmingham, Birmingham, AL, USA*
[6]*Department of Radiology, University of Alabama at Birmingham, Birmingham, AL, USA*
[7]*Departments of Otolaryngology, Neurosurgery, and Radiology, The University of Alabama at Birmingham, 1670 University Blvd., Birmingham, AL, 35294, USA*

Abstract

Purpose: Intraoperative optical imaging to guide surgeons during oncologic resections offers a unique and promising solution to the ambiguity of cancer margins to tactile and visual assessment that results in devastatingly high rates of positive margins. Sequestering of labeled antibodies by normal tissues with high expression of the antibody target, or "antigen sinks", diminishes the efficacy of these probes to provide contrast between the tumor and background tissues by decreasing the amount of circulating probe available for uptake by the tumor and by increasing the fluorescence of non-tumor tissues. We hypothesized that administering a dose of unlabeled antibody prior to infusion of the near-infrared (NIR) fluorescently labeled antibody would improve tumor-specific uptake and contrast of the fluorescently labeled probe by occupying extra-tumoral binding sites, thereby increasing the amount of labeled probe available for uptake by the tumor.

Procedures: In this study, we explore this concept by testing two different "pre-load" doses of unlabeled cetuximab (the standard 10-mg test dose, and a larger, experimental 100-mg test dose) in six patients receiving cetuximab conjugated to the fluorescent dye IRDye800CW (cetuximab-IRDye800CW) in a clinical trial, and compared the amount of fluorescent antibody in tumor and background tissues, as well as the tumor-specific contrast of each.

Results: The patients receiving the larger preload (100 mg) of unlabeled cetuximab demonstrated significantly higher concentrations (9.5 vs. 0.1 μg) and a longer half-life (30.3 vs. 20.6 days) of the labeled cetuximab in plasma, as well as significantly greater tumor fluorescence (32.3 vs. 9.3 relative fluorescence units) and tumor to background ratios (TBRs) (5.5 vs. 1.7).

Conclusions: Administering a preload of unlabeled antibody prior to infusion of the fluorescently labeled drug may be a simple and effective way to improve the performance of antibody-based probes to guide surgical resection of solid malignancies.

Correspondence to: Jason Warram; *e-mail:* mojack@uab.edu

Key words: Fluorescence-guided surgery, Loading dose, Cetuximab, Cetuximab-IRDye800CW, Head and neck cancer, Optical surgical navigation, Unlabeled preload

Introduction

The margins of solid malignancies are ambiguous and difficult for even the most experienced surgeons to identify by tactile and visual assessment alone during surgical resection. Incomplete tumor resections with positive margins are common, approaching 50 % in some cancer types, and are correlated with locoregional recurrence and poor patient outcomes [1–3]. Fluorescence-guided surgery has already been shown to increase the rate of complete resections and improve oncologic and functional outcomes [4, 5], and a wealth of pre-clinical data and clinical trials predicts the impending widespread implementation of this technology into the operating room [6–18]. While a number of fluorescent constructs are being explored, fluorescently labeled antibodies targeting cancer-specific markers are perhaps the most studied, with probes targeting human epidermal growth factor receptor 1 (EGFR) [19] and 2 (HER2) [20, 21], vascular endothelial growth factor (VEGF) [19, 20], carcinoembryonic antigen (CEA) [22], carbohydrate (cancer) antigen 19-9 (CA19-9) [23], and receptor tyrosine kinase (KIT) [24] and others utilized in a variety of cancer types [6]. Importantly, there are currently multiple clinical trials ongoing using fluorescently labeled antibodies to image cancer (NCT02113202, NCT01972373, NCT02129933, NCT01508572, NCT01987375, NCT02736578, NCT02415881) [6].

Antibodies are desirable vectors to carry fluorescent molecules to cancerous tissue for a number of reasons. The toxicity of systemically administered antibodies is generally low and adverse side effects are rarely severe [25–27]. Importantly, antibodies exhibit active and specific targeting of cancer receptors [25, 28], as compared to the non-binding mechanism of enhanced permeability and retention (EPR) utilized by other fluorescent probes [29, 30]. The long elimination half-lives of antibodies result in increased time for tumor exposure and uptake [26, 31], in contrast to smaller fluorescent probes that are often cleared too quickly and with suboptimal target binding [32]. The structure of antibodies is highly amenable to chemical manipulation, and the large number of active binding sites present on each provides an optimal scaffold for conjugating multiple fluorescent molecules [33, 34]. Given their increasing use as therapeutics, many antibodies have pre-existing FDA approval for human use and well-established patient safety profiles [25, 27, 28, 31], which can ease and expedite their clinical translation as imaging agents [6]. Finally, the over expression of antibody targets is often found in more than one tumor type, affording the opportunity for a single fluorescently labeled antibody for multiple cancer types.

However, experience with the pharmacokinetics and pharmacodynamics of antibodies offers insight into the potential complications of using fluorescently labeled antibodies to provide tumor-specific contrast during surgery. While tumors may overexpress antibody targets, these receptors are also endogenously expressed, sometimes ubiquitously, in many non-cancerous tissues, leading to off-target binding [25, 31, 35]. Cetuximab, the well-known anti-EGFR antibody used for treatment of various cancers, demonstrates high levels of binding to especially EGFR-rich tissues, including the skin and liver [27, 31, 35]. This target-mediated elimination, involving target receptor binding, internalization, and degradation, is the primary elimination route for many antibodies, including cetuximab, and is largely responsible for the nonlinear elimination kinetics they exhibit [25, 27, 28, 31, 35–37]. Additionally, the accumulation of circulating labeled antibodies by normal tissues occurs more rapidly than in tumor tissue, which has slower uptake kinetics due to inherently immature vascularization and elevated interstitial pressures [25, 28, 35]. Antibodies are also metabolized, although in less significant quantities, by cells of the reticuloendothelial system (RES) and by non-specific phagocytosis [25, 31, 36]. Sequestering of labeled antibodies by these off-target sites may negatively affect the tumor specific contrast by decreasing the amount of circulating probe available for tumor uptake and by increasing the fluorescence of non-tumor background tissues.

Although rare, the possibility of serious hypersensitivity and infusion reactions is another potential disadvantage to using antibodies as fluorescence vectors [26, 27, 37]. For cetuximab, this reaction rate ranges from 3 to 20 % depending on the geographic location [38]. In order to screen for individuals who may develop a serious adverse reaction to cetuximab, a small “test dose” is routinely administered prior to infusion of the full treatment dose (250 mg/m^2) in patients undergoing antibody-based cancer therapy [31, 37]. Based on this premise, patients recruited to be included in the study were administered an intravenous test dose of unlabeled (nonfluorescently tagged) cetuximab (10 or 100 mg) prior to infusion of cetuximab conjugated to the near-infrared (NIR) fluorescent dye IRDye800CW (cetuximab-IRDye800CW) so that any immune responses to the cetuximab could be identified prior to the study drug infusion. Two patients exhibited reactions to the test dose and were therefore unable to participate in the study [8]. While identifying hypersensitivity reactions was the driving force for the test dose administration, we hypothesized that the unlabeled antibody dose given first would also improve

tumor-specific uptake and contrast in the tumor, by saturating the EGFR in normal tissues with the unlabeled antibody. In this study, we explore this concept by testing two different "preload" doses of unlabeled cetuximab in six patients that subsequently received cetuximab-IRDye800CW during a clinical trial evaluating the safety and specificity of cetuximab-IRDye800CW in patients with head and neck squamous cell carcinoma (HNSCC) [8]. We then compared the amount of circulating fluorescent antibody, tumor and normal tissue fluorescence, and the tumor-specific contrast of each preload dose cohort.

Methods

Study Design

Tissue imaging and blood plasma were collected by the ablative surgeon from six consented patients enrolled in a clinical trial (Clinicaltrials.gov Identifier: NCT01987375) evaluating the safety and tumor specificity of systemically injected cetuximab-IRDye800CW (25 mg/m^2) for surgical navigation in patients with HNSCC, as previously reported [8]. For this study, 1 h prior to cetuximab-IRDye800CW infusion, patients (n = 3) received either the10-mg unlabeled cetuximab, per standard of care, or a 100-mg unlabeled cetuximab. Per trial design, patients then received 1 h infusion of cetuximab-IRDye800CW 3–4 days prior to the scheduled surgical procedure. Informed consent was obtained from all individual participants included in the study [8]. All patient data were anonymized and all experiments using the specimens were conducted in accordance with the rules and regulations approved by the University of Alabama Institutional Review Board.

Plasma Analysis

Pharmacokinetic assessments were performed prior to infusion, 2 h, 24 h, day 3, day 4, day 15, and day 30, post cetuximab-IRDye800CW infusion as previously described [39]. Aliquots of plasma samples (2.5 µl) were mixed with 4× sample buffer and resolved by NuPAGE 4–12 % Bis-Tris gel (Invitrogen Corporation; Carlsbad, CA). A known amount of cetuximab-IRDye800CW was assessed by gel electrophoresis and imaged at 800 nm (Pearl Impulse) to verify cetuximab-IRDye800CW at the 150 kDa protein marker. For each cohort, total milligram of cetuximab-IRDye800CW was calculated at each time point after quantification using Image Studio software (LI–COR Biosciences). Mean fluorescence intensity from size-matched ROIs was recorded and the milligram of cetuximab-IRDye800CW contained in each band was calculated based on mean counts from a set of cetuximab-IRDye800CW standards. Total plasma milligram of cetuximab-IRDye800CW at each time point for each 2.5-µl plasma sample was determined based on patient dose and total body blood weight. Total plasma values were averaged across patients for each cohort at every time point, and a scatter plot was generated to determine plasma clearance of cetuximab-IRDye800CW.

Optical Imaging

The LUNA imaging system (Novadaq, Toronto, Ontario, Canada) was used to acquire open-field, near-infrared fluorescence images of the primary tumor site (oral cavity or cutaneous), ipsilateral neck, forearm, and oral mucosa in the pre-operative clinic 2-h post-injection of cetuximab-IRDye800CW (day 0) followed by daily imaging and prior to resection on the day of surgery (day 3 or 4 post-infusion) [8]. Image settings were constant throughout acquisition with the camera at a constant distance of 30 cm.

Fluorescence Analysis

Fluorescence was quantified using integrated instrument software, SpyQ version 1.2 (Novadaq, Toronto, Ontario, Canada). Relative fluorescence units (RFU) were measured for tumor and background (approximately 3 to 4 cm from the edge of gross tumor) and averaged among six individual frames per imaging time point. Tumor-to-background ratio (TBR) was calculated by dividing tumor RFU by respective background RFU as previously described [40].

Results

In order to elucidate the effects of unlabeled cetuximab on tissue uptake of the fluorescent probe cetuximab-IRDye800CW, six patients with HNSCC enrolled in a clinical trial evaluating the safety and specificity of the probe were given either a 10- or 100-mg dose of unlabeled cetuximab prior to administration of the study drug. Fluorescence-imaging with an open-field NIR imaging device (LUNA) was used to evaluate the fluorescence of tumor and background tissue at several time points before and after drug administration. Samples of patient plasma were also collected and used to determine the amount of cetuximab-IRDye800CW in each sample at each time point. Table 1 displays the key characteristics of patients in each of the two pre-treatment dose cohorts. Both of the cohorts were comprised of two male patients and one female patient. The average age was 62 for the 100-mg cohort and 57 for the 10-mg cohort. There were two oral cavity tumors and one cutaneous tumor in each cohort. All patients received 25 mg/m^2 of cetuximab-IRDye800CW; therefore, there was no significant difference (P = 0.8) between the dose of cetuximab-IRDye800CW in cohort 1 (49.6 mg) and cohort 2 (48 mg).

Figure 1 depicts the average amount of cetuximab-IRDye800CW detected in the blood plasma of patients in

Table 1. Patient characteristics. Age, sex, primary tumor site, and dose of cetuximab-IRDye800CW for each patient in the two unlabeled cetuximab preload dose cohorts (100 and 10 mg)

Unlabeled cetuximab dose (mg)	Patient number	Age	Sex	Cancer site	Cetuximab-IRDye800CW dose (mg)
Cohort 1	1	77	M	Oral cavity	44.5
100 mg	2	40	M	Oral cavity	59.0
	3	69	F	Cutaneous	45.5
Cohort 2	4	69	F	Oral cavity	52.0
10 mg	5	38	M	Oral cavity	45.0
	6	64	M	Cutaneous	47.0

each unlabeled dose cohort (10 or 100 mg) at each collection time point over 15 days. There was no significant difference between the two cohorts on day 0 (100 mg = 51.18 μg ± 6.7, 10 mg = 41.23 μg ± 14.8, $P = 0.17$), which represented the peak amount of labeled drug detected in the plasma for both cohorts. However, there was significantly ($P < 0.05$) more cetuximab-IRDye800CW in the plasma of patients receiving the 100-mg unlabeled preload compared to those receiving the 10-mg unlabeled preload dose 1, 3, and 4 days post-infusion. On day 1 post-infusion, the average amount of cetuximab-IRDye800CW in patients receiving the 100-mg preload was 34.5 μg (± 10.7), and only 18.3 μg (± 6.1) in the 10-mg preload cohort ($P = 0.04$). On day 3 post-infusion, 14.3 μg (±1.5) cetuximab-IRDye800CW was detected in the plasma of patients given the 100-mg loading dose and nearly one third of that amount in the plasma of patients receiving the 10-mg loading dose (5.7 μg ± 5.3, $P = 0.03$). The greatest difference in the amount of cetuximab-IRDye800CW detected in the plasma of patients in the two cohorts occurred on day 4 post-infusion. Those patients in the 100-mg preload cohort had an average of 9.5 μg (± 4.2) cetuximab-IRDye800CW in the plasma, while the labeled drug had dropped to nearly undetectable amounts in those patients who received the 10-mg loading dose (0.1 μg ± 0.12, $P = 0.008$). No patient from either cohort had detectable levels of the labeled cetuximab in the plasma on days 15 or 30 post-infusion.

Figure 1 also illustrates that the rate of clearance of the cetuximab-IRDye800CW from the plasma was less in patients who received the 100-mg preload of unlabeled cetuximab compared to those who received the 10-mg preload. The average half-life of cetuximab-IRDye800CW for the 100-mg preload cohort was 30.33 h (±7.3), which was significantly longer than that of the 10-mg preload cohort (20.6 h ± 4.0, $P = 0.05$).

Figure 2 demonstrates the average fluorescence of the forearm skin, oral mucosa, and tumor tissue of the patients in the 100-mg preload group compared to the 10-mg preload group at the day of infusion of cetuximab-IRDye800CW (day 0), day 1 post-infusion, and day 3 or 4 post-infusion (day of surgery). There was no significant difference between the average tissue fluorescence of the oral mucosa in patients receiving the 10-mg preload dose and those given 100 mg of unlabeled cetuximab at any of the imaging time points (Fig. 2a). The mean fluorescence of the skin of patients in the 10-mg preload dose cohort was significantly greater than that of patients in the 100-mg cohort on day 1 post-infusion ($P = 0.007$). However, there was no significant difference in mean fluorescence of patient skin between the two cohorts on day 0 or on the day of surgery (Fig. 2b). Figure 2c demonstrates that the average fluorescence of tumor tissue in the 100-mg preload cohort (32.3 RFU ± 18.8) was significantly greater than the tumor fluorescence of the 10-mg preload cohort (9.3 ± 4.9) on the day of surgery ($P = 0.05$).

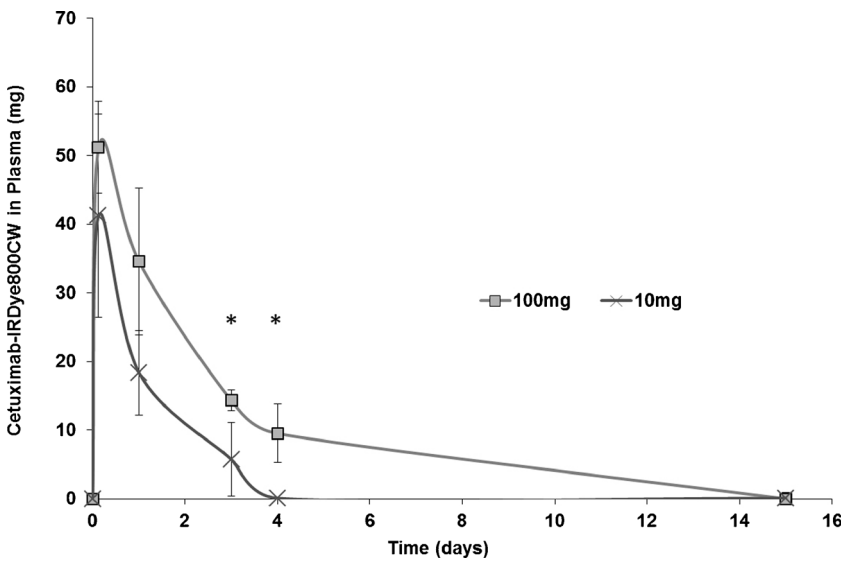

Fig. 1. Plasma pharmacokinetics of cetuximab-IRDye800CW**.** Average amount of cetuximab-IRDye800CW detected in 2.5 μl of blood plasma for patients in each unlabeled pre-treatment dose cohort (10 or 100 mg) at each collection time point over 15 days.

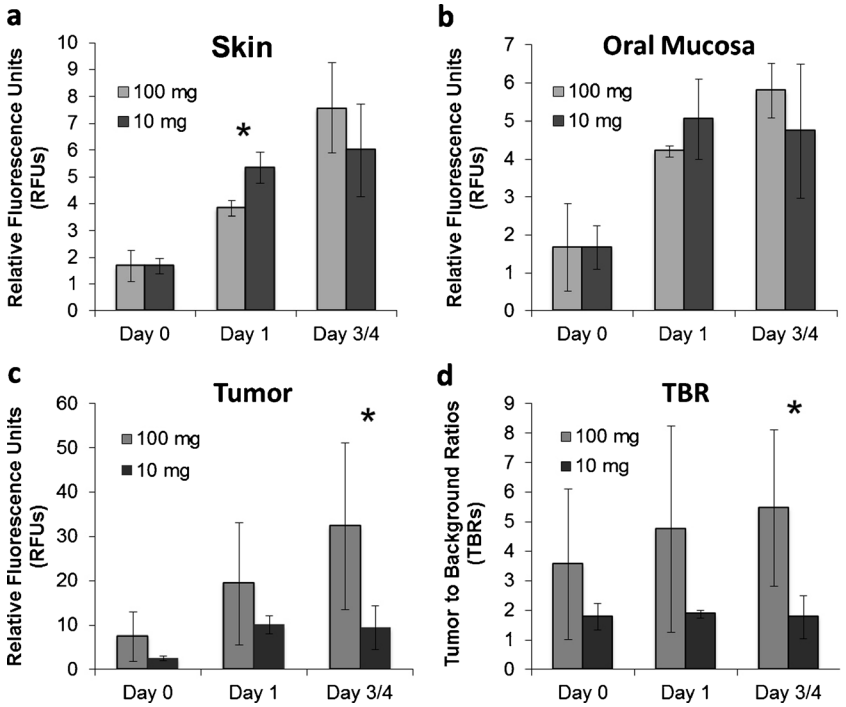

Fig. 2. Tissue fluorescence. Average fluorescence (relative fluorescence units) of patient's **a** skin, **b** oral mucosa, **c** tumor tissue, and **d** the tumor to background ratios for each unlabeled pre-treatment dose cohort (10 or 100 mg) at day 0, 1, and 3 or 4 (day of surgery).

Finally, Fig. 2d depicts the trending increase in the TBR for the 100-mg preload cohort over time compared to the stable contrast ratio of the 10-mg preload cohort (1.7, 1.8, and 1.7 on day 0, 1, and 3 or 4, respectively). The mean TBR was more than twofold greater for the 100-mg preload dose cohort (5.5 ± 2.6) than for the 10-mg cohort (1.7 ± 0.7) on the day of surgery ($P = 0.04$).

Discussion

Fluorescence-guided surgery is a promising technique to guide the surgical resection of solid malignancies, and antibodies have been shown to be an effective imaging agent in humans [6, 8]. However, sequestration of these antibodies by non-tumor tissues endogenously expressing the target receptor may decrease antibody bioavailability and tumor-specific binding. This concept is commonly utilized in the field of radioimmunotherapy, in which a "cold" preload dose of unlabeled antibody is used to improve the bioavailability and targeting of subsequently administered radiolabeled antibodies intended to eradicate a malignant target [41, 42]. We evaluated the effects of unlabeled cetuximab preloading on the pharmacokinetics and tumor targeting of systemically injected cetuximab-IRDye800CW in human patients with HNSCC.

Patients who received the larger unlabeled preload dose (100 mg) demonstrated greater peak concentrations and a longer half-life of the cetuximab-IRDye800CW in blood plasma. Importantly, almost no circulating labeled drug was present in the plasma in the 10-mg preload cohort at the time of surgery, while the plasma of patients in the 100-mg preload cohort contained nearly 100 times more labeled drug at that time. It is likely that this increase in the amount of circulating cetuximab-IRDye800CW and its longer biological half-life in the 100-mg cohort was the result of increased off-target receptor occupancy and tissue sequestration by the larger dose of unlabeled antibody preload, substantially increasing the uptake of the cetuximab-IRDye800CW in tumor. One study using radiolabeled antibodies observed similar results, noting a significant increase in the concentration and resident time in the blood stream of the radiolabeled antibody when preload dose of unlabeled antibody was used [42].

It is important to note that the highest preload dose used in this study (100 mg) is only a fraction of the therapeutic dose of cetuximab (250 mg/m^2) [31, 37]. One patient from the 10-mg dose cohort experienced adverse side effects possibly attributable to the study (dizziness, electrocardiogram changes, tumor pain, and hypomagnesemia), as did one patient from the 100-mg dose cohort (electrocardiogram changes, elevated aspartate aminotransferase, and hypomagnesemia) [8]. In both cases, the change on the electrocardiogram was a prolongation of the QTc interval, and paired *t* tests demonstrated no significant prolongation from baseline in either case [8]. All adverse events were grade 1 and resolved by the conclusion of the trial [8]. No increase in adverse events occurred in the group receiving the larger preload dose, suggesting that a preload of at least 100 mg can be administered without increased toxicity. It is also important to note that, even when a larger preload was used,

there was no detectable cetuximab-IRDye800CW in patients in either cohort at days 15 and 30, meaning that this increase in half-life does not risk patient safety by prolonging drug circulation beyond expected time frames in immunotherapy.

Furthermore, there was no significant difference in patient age, weight, or cetuximab-IRDye800CW dose between the two cohorts, and the groups were matched for gender and primary tumor location. While statistical power was limited by the number of patients, these findings suggest that the significant increase in the TBRs of patients who received the 100-mg dose is unlikely to be an artifact of these confounding variables. Additionally, the findings in this study are not likely due to differences in EGFR expression of the tumors, as a separate analysis of tumor tissue of the patients in this clinical trial found no significant difference in EGFR expression between cohorts [43]. Thus, this significant difference in the pharmacokinetics and TBRs between the two preload dose cohorts is most likely attributable to the difference in the unlabeled preload dose.

In conclusion, this study conducted in humans with SCC of the head and neck found that administration of a 100-mg preload dose of unlabeled cetuximab prior to systemically injected cetuximab-IRDye800CW yielded slower plasma clearance and increased tumor-specific uptake of the fluorescently labeled drug, as well as improved fluorescence contrast when compared to the standard 10-mg preload dose. These findings were consistent with a number of radioimmunotherapy studies that found increased tumor-specific uptake of radiolabeled antibodies following a "cold" preload dose [41, 42, 44].

To the best of our knowledge, this is the first study comparing the effects of different preload doses of an unlabeled antibody on the performance of the fluorescently labeled antibody as an optical contrast agent to guide oncologic surgical resection. This study was limited by the small number of patients, a constraint inherent to the standard "3 + 3" dose-escalation study design of the overarching clinical trial. In order to draw definitive conclusions about the optimal preload of unlabeled antibodies in antibody-based fluorescence-guided surgery, larger studies testing a range of preload doses should be conducted, as has been done with radioimmunotherapy [41, 45]. Also, given the variability among different antibodies and their target receptors, conclusions should be limited to the specific antibody investigated. However, this study offers valuable insight into the potential for a preload of unlabeled antibody to improve the bioavailability and performance of antibody-based fluorescent probes to navigate the surgical resection of solid malignancies.

Conclusion

Fluorescence-guided surgery is a promising technique but in order to maximize the efficiency of fluorescent probes, efforts must be made to improve tumor-specific uptake of the probe. This study demonstrated enhanced pharmacokinetics, increased tumor-specific uptake, and improved optical contrast of fluorescently labeled cetuximab in patients with HNSCC when a preload of 100-mg unlabeled (nonfluorescent) antibody was administered, compared with 10 mg. While further studies and dose-range testing must be done to validate the efficacy of this technique, this strategy may provide a simple method for improving the performance of antibody-based fluorescence probes to guide oncologic resections without adding a substantial burden to the approval process.

Acknowledgments. The authors acknowledge Ms. Yolanda Hartman and Ms. Lisa Clemons for their contributions to this manuscript.

Compliance with Ethical Standards

Conflict of Interest

The authors declare that they have no conflict of interest.

Funding

Funding for this manuscript includes the Robert Armstrong Research Acceleration Fund, the UAB Comprehensive Cancer Center, NIH/NCI (R21CA179171, R21CA182953, T32CA091078), and institutional equipment loans from Novadaq and LI-COR Biosciences.

References

1. Woolgar JA, Triantafyllou A (2005) A histopathological appraisal of surgical margins in oral and oropharyngeal cancer resection specimens. Oral Oncol 41:1034–1043
2. McMahon J, O'Brien CJ, Pathak I et al (2003) Influence of condition of surgical margins on local recurrence and disease-specific survival in oral and oropharyngeal cancer. Br J Oral Maxillofac Surg 41:224–231
3. Hinni ML, Ferlito A, Brandwein-Gensler MS et al (2013) Surgical margins in head and neck cancer: a contemporary review. Head Neck 35:1362–1370
4. Stummer W, Novotny A, Stepp H et al (2000) Fluorescence-guided resection of glioblastoma multiforme by using 5-aminolevulinic acid-induced porphyrins: a prospective study in 52 consecutive patients. J Neurosurg 93:1003–1013
5. Stummer W, Pichlmeier U, Meinel T et al (2006) Fluorescence-guided surgery with 5-aminolevulinic acid for resection of malignant glioma: a randomised controlled multicentre phase III trial. Lancet Oncol 7:392–401
6. Rosenthal EL, Warram JM, de Boer E et al (2016) Successful translation of fluorescence navigation during oncologic surgery: a consensus report. J Nucl Med 57:144–150
7. Koch M, Ntziachristos V (2016) Advancing surgical vision with fluorescence imaging. Annu Rev Med 67:153–164
8. Rosenthal EL, Warram JM, de Boer E et al (2015) Safety and tumor specificity of cetuximab-IRDye800 for surgical navigation in head and neck cancer. Clin Cancer Res 21:3658–3666
9. Whitley MJ, Cardona DM, Lazarides AL et al (2016) A mouse-human phase 1 co-clinical trial of a protease-activated fluorescent probe for imaging cancer. Sci Transl Med 8:320ra324
10. Day KE, Sweeny L, Kulbersh B et al (2013) Preclinical comparison of near-infrared-labeled cetuximab and panitumumab for optical imaging of head and neck squamous cell carcinoma. Mol Imaging Biol 15:722–729
11. Korb ML, Hartman YE, Kovar J et al (2014) Use of monoclonal antibody-IRDye800CW bioconjugates in the resection of breast cancer. J Surg Res 188:119–128
12. Day KE, Beck LN, Deep NL et al (2013) Fluorescently labeled therapeutic antibodies for detection of microscopic melanoma. Laryngoscope 123:2681–2689
13. Kulbersh BD, Duncan RD, Magnuson JS et al (2007) Sensitivity and specificity of fluorescent immunoguided neoplasm detection in head

and neck cancer xenografts. Arch Otolaryngol Head Neck Surg 133:511–515
14. Rosenthal EL, Kulbersh BD, Duncan RD et al (2006) In vivo detection of head and neck cancer orthotopic xenografts by immunofluorescence. Laryngoscope 116:1636–1641
15. Tanaka E, Choi HS, Humblet V et al (2008) Real-time intraoperative assessment of the extrahepatic bile ducts in rats and pigs using invisible near-infrared fluorescent light. Surgery 144:39–48
16. Tanaka E, Ohnishi S, Laurence RG et al (2007) Real-time intraoperative ureteral guidance using invisible near-infrared fluorescence. J Urol 178:2197–2202
17. van der Vorst JR, Schaafsma BE, Verbeek FP et al (2013) Near-infrared fluorescence sentinel lymph node mapping of the oral cavity in head and neck cancer patients. Oral Oncol 49:15–19
18. Hutteman M, Choi HS, Mieog JS et al (2011) Clinical translation of ex vivo sentinel lymph node mapping for colorectal cancer using invisible near-infrared fluorescence light. Ann Surg Oncol 18:1006–1014
19. Tjalma JJ, Garcia-Allende PB, Hartmans E et al (2016) Molecular fluorescence endoscopy targeting vascular endothelial growth factor A for improved colorectal polyp detection. J Nucl Med 57:480–485
20. Terwisscha van Scheltinga AG, van Dam GM, Nagengast WB et al (2011) Intraoperative near-infrared fluorescence tumor imaging with vascular endothelial growth factor and human epidermal growth factor receptor 2 targeting antibodies. J Nucl Med 52:1778–1785
21. Wu J, Ma R, Cao H et al (2013) Intraoperative imaging of metastatic lymph nodes using a fluorophore-conjugated antibody in a HER2/neu-expressing orthotopic breast cancer mouse model. Anticancer Res 33:419–424
22. Metildi CA, Kaushal S, Pu M et al (2014) Fluorescence-guided surgery with a fluorophore-conjugated antibody to carcinoembryonic antigen (CEA), that highlights the tumor, improves surgical resection and increases survival in orthotopic mouse models of human pancreatic cancer. Ann Surg Oncol 21:1405–1411
23. McElroy M, Kaushal S, Luiken GA et al (2008) Imaging of primary and metastatic pancreatic cancer using a fluorophore-conjugated anti-CA19-9 antibody for surgical navigation. World J Surg 32:1057–1066
24. Metildi CA, Tang CM, Kaushal S et al (2013) In vivo fluorescence imaging of gastrointestinal stromal tumors using fluorophore-conjugated anti-KIT antibody. Ann Surg Oncol 20(Suppl 3):S693–S700
25. Keizer RJ, Huitema AD, Schellens JH, Beijnen JH (2010) Clinical pharmacokinetics of therapeutic monoclonal antibodies. Clin Pharmacokinet 49:493–507
26. Wang W, Wang EQ, Balthasar JP (2008) Monoclonal antibody pharmacokinetics and pharmacodynamics. Clin Pharmacol Ther 84:548–558
27. Mould DR, Green B (2010) Pharmacokinetics and pharmacodynamics of monoclonal antibodies: concepts and lessons for drug development. BioDrugs 24:23–39
28. Dostalek M, Gardner I, Gurbaxani BM et al (2013) Pharmacokinetics, pharmacodynamics and physiologically-based pharmacokinetic modelling of monoclonal antibodies. Clin Pharmacokinet 52:83–124
29. Greish K (2007) Enhanced permeability and retention of macromolecular drugs in solid tumors: a royal gate for targeted anticancer nanomedicines. J Drug Target 15:457–464
30. Greish K (2010) Enhanced permeability and retention (EPR) effect for anticancer nanomedicine drug targeting. Methods Mol Biol 624:25–37
31. Mould DR, Sweeney KR (2007) The pharmacokinetics and pharmacodynamics of monoclonal antibodies—mechanistic modeling applied to drug development. Curr Opin Drug Discov Devel 10:84–96
32. Owens EA, Lee S, Choi J, Henary M, Choi HS (2015) NIR fluorescent small molecules for intraoperative imaging. Wiley Interdiscip Rev Nanomed Nanobiotechnol 7:828–838
33. Vira S, Mekhedov E, Humphrey G, Blank PS (2010) Fluorescent-labeled antibodies: balancing functionality and degree of labeling. Anal Biochem 402:146–150
34. McCombs JR, Owen SC (2015) Antibody drug conjugates: design and selection of linker, payload and conjugation chemistry. AAPS J 17:339–351
35. Lammerts van Bueren JJ, Bleeker WK, Bogh HO et al (2006) Effect of target dynamics on pharmacokinetics of a novel therapeutic antibody against the epidermal growth factor receptor: implications for the mechanisms of action. Cancer Res 66:7630–7638
36. Ternant D, Bejan-Angoulvant T, Passot C et al (2015) Clinical pharmacokinetics and pharmacodynamics of monoclonal antibodies approved to treat rheumatoid arthritis. Clin Pharmacokinet 54:1107–1123
37. Harding J, Burtness B (2005) Cetuximab: an epidermal growth factor receptor chemeric human-murine monoclonal antibody. Drugs Today (Barc) 41:107–127
38. Adams CB, Street DS, Crass M, Bossaer JB (2015) Low rate of cetuximab hypersensitivity reactions in Northeast Tennessee: An Appalachian effect? J Oncol Pharm Pract
39. Zinn KR, Korb M, Samuel S et al (2015) IND-directed safety and biodistribution study of intravenously injected cetuximab-IRDye800 in cynomolgus macaques. Mol Imaging Biol 17:49–57
40. Heath CH, Deep NL, Beck LN et al (2013) Use of panitumumab-IRDye800 to image cutaneous head and neck cancer in mice. Otolaryngol Head Neck Surg 148:982–990
41. Kletting P, Meyer C, Reske SN, Glatting G (2010) Potential of optimal preloading in anti-CD20 antibody radioimmunotherapy: an investigation based on pharmacokinetic modeling. Cancer Biother Radiopharm 25:279–287
42. Muylle K, Flamen P, Vugts DJ et al (2015) Tumour targeting and radiation dose of radioimmunotherapy with (90)Y-rituximab in CD20+ B-cell lymphoma as predicted by (89)Zr-rituximab immuno-PET: impact of preloading with unlabelled rituximab. Eur J Nucl Med Mol Imaging 42:1304–1314
43. de Boer E, Warram JM, Tucker MD et al (2015) In vivo fluorescence immunohistochemistry: localization of fluorescently labeled cetuximab in squamous cell carcinomas. Sci Rep 5:10169
44. Garkavij M, Tennvall J, Strand SE et al (1994) Improving radioimmunotargeting of tumors: the impact of preloading unlabeled L6 monoclonal antibody on the biodistribution of 125I-L6 in rats. J Nucl Biol Med 38:594–600
45. Kletting P, Kull T, Bunjes D et al (2011) Optimal preloading in radioimmunotherapy with anti-cD45 antibody. Med Phys 38:2572–2578